

Very forward inclusive jet cross sections in p+Pb collisions at $\sqrt{s_{NN}} = 5.02$ TeV at CMS

Merijn H F van de Klundert on behalf of the CMS collaboration*

University of Antwerp (BE)

E-mail: mhfvandeklundert@gmail.com

Very forward inclusive jet energy spectra were measured with the CMS experiment at the LHC in proton-lead collisions, with a centre-of-mass energy of $\sqrt{s_{NN}} = 5.02$ TeV. The measurement was performed using the CASTOR calorimeter, which measures in the pseudorapidity range $-6.6 < \eta < -5.2$. The spectra, with the proton (p+Pb) or ion (Pb+p) towards CASTOR, are unfolded to the particle level and compared to predictions of various event generators. The p+Pb/Pb+p ratio of the spectra is also presented, for which the systematic uncertainties in the measurement are significantly reduced. The event generators considered in this analysis are not able to describe any of the spectra in their full energy range. Deviations between data and the models in excess of two orders of magnitude are observed.

25th International Workshop on Deep Inelastic Scattering and Related Topics

3-7 April 2017

University of Birmingham, Birmingham, UK

*Speaker.

1. Introduction

A key argument for colliding protons with lead ions at the LHC is the search for signals of nonlinear QCD, which is expected to lead to saturation of the gluon density and a specific description of its evolution. Beside a major research topic in its own right, gluon saturation is also an important theoretical ingredient for formulating predictions on the initial state of heavy ion collisions.

Nonlinear effects are expected to become significant at large parton densities. These large densities can be found for gluons carrying a small fraction x of the longitudinal momentum of the hadron. It is expected that nonlinear gluon fusion is enhanced for heavy ions, since the gluon density in a heavy ion is larger than in a proton. The x value of the parton can approximately be reconstructed from the jet and beam kinematics via:

$$x = \frac{p_T \cdot e^{-|\eta|}}{\sqrt{s}}. \quad (1.1)$$

Therefore, optimal sensitivity to saturation can be achieved by measuring low transversal momentum p_T jets in the forward direction in proton-lead collisions.

We present an analysis of such a measurement in the pseudorapidity range $-6.6 < \eta < -5.2$, in proton-lead collisions with a centre-of-mass energy of $\sqrt{s_{NN}} = 5.02$ TeV. In this document we'll refer generally to proton-lead collision as $p+Pb$ collisions for brevity; with this both type of collisions with the proton ($p+Pb$) or the ion ($Pb+p$) to CASTOR are implied, unless we refer specifically to results for a particular beam configuration.

Finally, it should be noted that the jet energy spectra and their ratio are presented in the lab frame, which is boosted with respect of the centre-of-mass frame (the proton beam had an energy of 4 TeV in the lab frame).

2. The CASTOR calorimeter at CMS

A detailed description of the CMS detector, together with a definition of the coordinate system used and the relevant kinematic variables, can be found in [1].

The central feature of the CMS apparatus is a superconducting solenoid of 6 m internal diameter, providing a magnetic field of 3.8 T. Within the solenoid volume are a silicon pixel and strip tracker, a lead tungstate crystal electromagnetic calorimeter (ECAL), and a brass and scintillator hadron calorimeter (HCAL), each composed of a barrel and two endcap sections. Forward calorimeters (HF) extend the pseudorapidity coverage provided by the barrel and endcap detectors. HF provides coverage in the range $3.0 < |\eta| < 5.2$. They also serve as luminosity monitors. The CASTOR calorimeter is the key detector of this analysis. It is a non-compensating electromagnetic-hadronic sampling Cherenkov calorimeter. Since it is installed at minus 14 m from the CMS interaction point at only 1 cm in the transversal plane from the beam pipe, it can perform a measurement in the very forward range $-6.6 < \eta < -5.2$.

CASTOR is mechanically organised into two halves. A half consists of eight sectors in the azimuthal plane (ϕ); it should be noted that CASTOR has no η segmentation though. Each sector is longitudinally segmented into 14 modules. Thus, CASTOR has 224 channels overall. The energy

deposits in the channels of a sector are summed into a tower, which has its η coordinate fixed to the geometrical centre of the sector. These towers are clustered in ϕ into CASTOR jets, using the anti- k_T [2] algorithm with a radius of 0.5. Due to the non-compensating nature of CASTOR, a correction is needed for the hadronic jets. Therefore, energy dependent calibration functions were derived from simulations and applied to the hadronic CASTOR jets. As a consequence, an additional systematic uncertainty due this procedure was added to the results.

On generator level, generally all stable particles for which $c \cdot \tau$ is larger than 10 mm are clustered into generator jets, using the same clustering algorithm.

The alignment and calibration of CASTOR are in particular important aspects of its performance, since these will contribute substantially to the systematic uncertainty. The position of CASTOR during the p+Pb data taking is known with an uncertainty of ~ 3 mm. CASTOR is intercalibrated by equalising the gains of its channels to the response of beam halo muons. The absolute calibration is performed by extrapolating a measurement of the η dependence of the energy deposit in the HF subsystem, leading to an uncertainty in the absolute calibration of 15%. A more detailed description of the performance of CASTOR during the p+Pb data taking and the sources of systematic uncertainty can be found at [3] and references therein.

3. Data and event selection

The p+Pb collisions were delivered to CMS at a centre-of-mass energy of $\sqrt{s_{NN}} = 5.02$ GeV in early 2013.

To select hadronic non-diffractive events, collisions were selected with an online minimum bias trigger. Offline, this was combined with the requirement of simultaneous activity in both HF calorimeters. The effect of pileup (multiple collisions per bunch crossing) in data was mitigated by analysing only events with maximally one good primary vertex. A consistent event selection was adopted on generator level.

The response of the CMS detector was simulated using GEANT4 software [4]. To accommodate for the alignment uncertainty of CASTOR, simulations were performed with CASTOR shifted maximally inwards and outwards with respect to the beampipe.

Three event generators are considered in this analysis: HIJING [5], EPOS-LHC [6], and QGSJETII-04 [7]. These generators do not include photon-induced events, and HIJING in addition does not include diffractive events. Events were simulated using these models to assess the uncertainty on the CASTOR jet response matrix, the non-matched generator jets (called misses), and the non-matched detector jets (called fakes), which are a prerequisite to correct the data back to the stable hadron level.

The hard interactions in HIJING are calculated using perturbative QCD, as implemented in PYTHIA [8]. It performs its parton evolution via DGLAP equations. Nuclear shadowing of the pdf of the ion is incorporated to account for the nuclear effects.

EPOS-LHC and QGSJETII-04 are both based on a mixture of the parton and Pomeron model. The interference of soft contributions with the hard interactions effectively leads to screening for EPOS-LHC, which qualitatively agrees with the concept of saturation.

QGSJETII-04 functions similarly to EPOS-LHC, but saturation is implemented via multi-Pomeron interactions.

4. Unfolding the inclusive CASTOR jet spectrum

The correction of the detector level CASTOR jet spectrum to a generator level jet spectrum is briefly explained in this section (a detailed discussion can be found at [3]). The correction relies on a precise estimate of the response of CASTOR to generator jets and the miss and fake rates. These were obtained from realistic event simulations.

The unfolding is performed by an implementation of the d'Agostini iterative procedure [9] in ROOUNFOLD [10]. A lower jet energy cutoff of 150 GeV was applied to the jets on detector level. The unfolded spectra however are considered reliable only above a jet energy cutoff of 600 GeV.

5. Results

The final unfolded spectra with their uncertainties are presented in Fig. 1 for p+Pb (left), Pb+p (middle), and p+Pb/Pb+p (right). Predictions from EPOS-LHC, HIJING, and QGSJETII-04 are included.

From both the graphs and table 1, which depicts the systematic uncertainties for the minimal and maximal jet energy bin, it can be seen that for p+Pb and Pb+p the dominant uncertainty in the data at low energies is caused by the model uncertainty, while at large energies the energy scale uncertainty is dominant. For p+Pb/Pb+p, this uncertainty largely cancels out and the model uncertainty is dominant instead.

The predictions of the models differ strongly for p+Pb collisions, exceeding two orders of magnitude at 2.5 TeV. HIJING describes the data very well, while EPOS-LHC and QGSJETII-04 appear to have a too soft spectrum.

For Pb+p collisions all models underestimate the data for a few lower energy bins. From approx. 1.2 TeV onwards, all models are in agreement with the data within the systematic uncertainty.

None of the models are able to describe the p+Pb/Pb+p ratio on the whole range. HIJING describes the shape well but is off in normalisation. It can be seen that for the ratio the high energy behaviour of HIJING does not describe the data due to the underestimation of the Pb+p data, while this could not be resolved for p+Pb or Pb+p individually; this is a clear virtue of the uncertainty cancellation. EPOS-LHC manages to describe the lower energy part of the ratio, but significantly fails to describe the shape of the ratio at high energies (due to the severe underestimation of p+Pb). QGSJETII-04 describes the shape of the data better than EPOS-LHC but describes the data overall worse, which can also be attributed to the predictions for p+Pb.

Similar conclusions can be drawn from the comparison of the spectra on detector level, depicted in Fig. 2. The systematic uncertainties are substantially reduced though, since no model uncertainty needed to be introduced. In particular the low energy behaviour of the models for Pb+p collisions can be more clearly distinguished from the data. For the ratio p+Pb/Pb+p the deviations between the data and the models are more pronounced due to the absence of the model uncertainty, which is dominant for the ratio on particle level. Also, the lower energy behaviour of EPOS-LHC and QGSJETII-04 can be seen in this plot not to describe the data well.

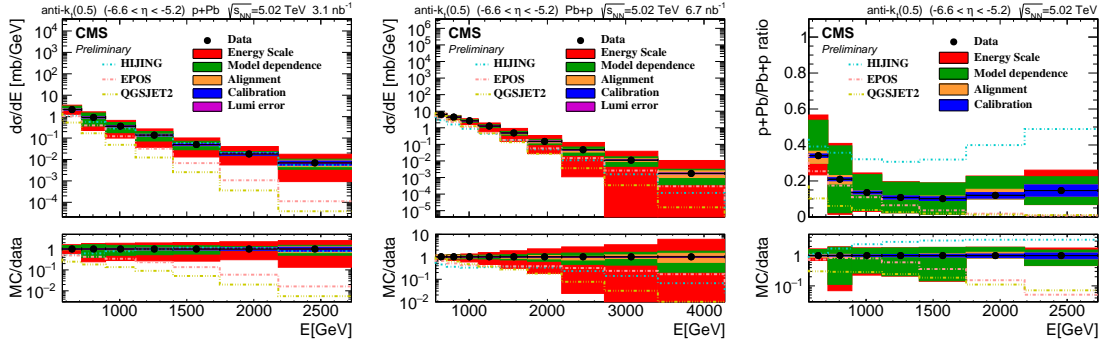


Figure 1: Differential CASTOR jet energy cross sections. The CASTOR jets were unfolded to a spectrum of particle level jets in the CASTOR acceptance ($-6.6 < \eta < -5.2$). Model predictions are included for EPOS-LHC, HIJING, and QGSJETII-04. Left: p+Pb collisions (with the proton towards CASTOR). Middle: Pb+p collisions (with the ion towards CASTOR). Right: the ratio of the cross sections for p+Pb/Pb+p. The figures are from [3].

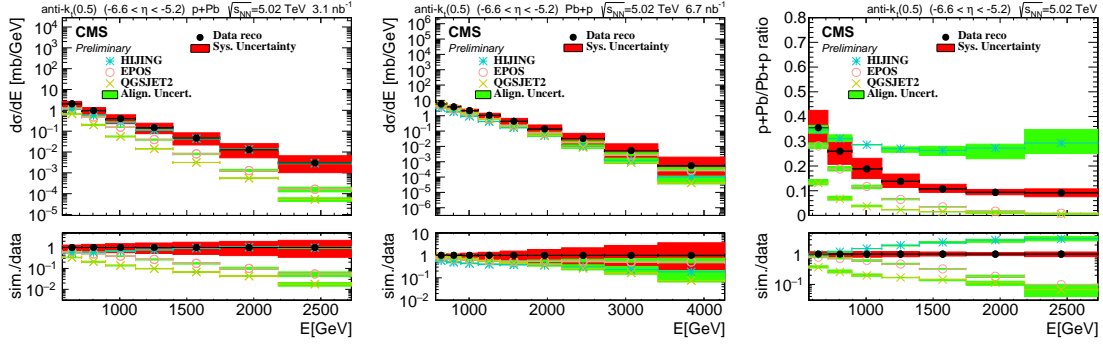


Figure 2: Differential CASTOR jet energy cross sections on detector level. Model predictions are included for EPOS-LHC, HIJING, and QGSJETII-04. Left: p+Pb collisions (with the proton towards CASTOR). Middle: Pb+p collisions (with the ion towards CASTOR). Right: the ratio of the cross sections for p+Pb/Pb+p. The figures are from [3].

Source uncertainty	p+Pb		Pb+p		p+Pb/Pb+p	
	600 GeV	2.5 TeV	600 GeV	2.5 TeV	600 GeV	2.5 TeV
Energy scale	+2%	+145%	+6%	+170%	+5%	+57%
	-2%	-71%	-6%	-82%	-7%	-9%
Model dependence	+14%	+37%	+13%	+46%	+24%	+48%
	-14%	-37%	-13%	-46%	-24%	-48%
Alignment	+3%	+24%	+3%	+49%	+10%	+4%
	-3%	-24%	-6%	-24%	-6%	-6%
Jet identification	+1%	+22%	<1%	<1%	+1%	+21%
	-1%	-22%	<1%	<1%	-1%	-21%
Total	+15%	+153%	+15%	+177%	+26%	+77%
	-14%	-87%	-16%	-98%	-26%	-54%

Table 1: The contribution of various sources to the systematic uncertainty in the highest and lowest common energy bin for the p+Pb, Pb+p, and p+Pb/Pb+p spectra. The overall number is also quoted. The numbers are from [3].

References

- [1] S. Chatrchyan et al. The CMS Experiment at the CERN LHC. *JINST*, 3:S08004, 2008.
- [2] Matteo Cacciari, Gavin P. Salam, and Gregory Soyez. The Anti-k(t) jet clustering algorithm. *JHEP*, 04:063, 2008.
- [3] CMS collaboration. Very forward inclusive jet cross sections in p+Pb collisions at $\sqrt{s_{NN}} = 5.02$ TeV. *CMS-PAS-FSQ-17-001*, 2017.
- [4] S. Agostinelli et. al. Geant4 a simulation toolkit. *Nuclear Instruments and Methods in Physics Research Section A: Accelerators, Spectrometers, Detectors and Associated Equipment*, 506(3):250 – 303, 2003.
- [5] Xin-Nian Wang and Miklos Gyulassy. hijing. *Phys. Rev. D*, 44:3501–3516, Dec 1991.
- [6] T. Pierog, Iu. Karpenko, J. M. Katzy, E. Yatsenko, and K. Werner. EPOS LHC: Test of collective hadronization with data measured at the CERN Large Hadron Collider. *Phys. Rev.*, C92(3):034906, 2015.
- [7] Ostapchenko, S. QGSJET-II: physics, recent improvements, and results for air showers. *EPJ Web of Conferences*, 52:02001, 2013.
- [8] Torbjörn Sjöstrand, Stefan Ask, Jesper R. Christiansen, Richard Corke, Nishita Desai, Philip Ilten, Stephen Mrenna, Stefan Prestel, Christine O. Rasmussen, and Peter Z. Skands. An introduction to pythia 8.2. *Computer Physics Communications*, 191:159 – 177, 2015.
- [9] G. D’Agostini. A Multidimensional unfolding method based on Bayes’ theorem. *Nucl. Instrum. Meth.*, A362:487–498, 1995.
- [10] Tim Adye. Unfolding algorithms and tests using RooUnfold. (arXiv:1105.1160):6 p, May 2011. Comments: 6 pages, 5 figures, presented at PHYSTAT 2011, CERN, Geneva, Switzerland, January 2011, to be published in a CERN Yellow Report.